Multiwave imaging of the Earth's subsurface : a laboratory scale feasibility study

Thomas Gallot, Alison Malcolm, Steve Brown, Dan Burns, and Michael FehlerThomas SzaboZhenya Zhu

Citation: Proc. Mtgs. Acoust. **16**, 045007 (2012); doi: 10.1121/1.4749271
View online: http://dx.doi.org/10.1121/1.4749271
View Table of Contents: http://asa.scitation.org/toc/pma/16/1
Published by the Acoustical Society of America

Proceedings of Meetings on Acoustics

Volume 16, 2012 http://acousticalsociety.org/

XVII International Conference on Nonlinear Elasticity in Materials
Cefalu, Sicily, Italy
1 - 7 July 2012
Session PA: Physical Acoustics

Multiwave imaging of the Earth's subsurface : a laboratory scale feasibility study

Thomas Gallot*, Alison Malcolm, Steve Brown, Dan Burns, Michael Fehler, Thomas Szabo and Zhenya Zhu

***Corresponding author's address: Department of Earth, Atmospheric and Planetary Sciences, Massachusetts Institute of Technology, 77 Massachusetts Avenue, Cambridge, MA 02139, gallott@mit.edu**

Multi-wave high resolution imaging methods have been developped in medical imaging. The feasibility of similar methods for geophysical applications has been studied. An interesting configuration is the subsurface imaging in a km scale where a compressional wavefield can be measured between 2 boreholes. A perturbation of this wavefield by shear waves created from the surface could creates a non-linear interaction. In this context, preliminary laboratory scale experiments have been performed in rocks (berea sandstones). The interaction between shear waves and compressional waves has been studied. The shear wave is generated by a shear transducer in the tens of kHz and used as a "localized pump". The localization of this pump is essential for a possible imaging application. The probe is a compressional pulse in the hundreds of kHz range. In this configuration, the delay of the ultrasounds pulse arrival, the time of flight modulation by nonlinear interaction is studied. Fast and slow nonlinear dynamics can be observed in this configuration. This experimental work is in progress.

Published by the Acoustical Society of America through the American Institute of Physics

 [DOI: 10.1121/1.4749271]
Received 31 Jul 2012; published 17 Aug 2012

Introduction

The basic idea behind multi-wave imaging is to use the mixing of different waves to create new imaging modalities. In medical imaging this concept has been developed to create enhanced contrast and resolution imaging systems. This work aims to apply these ideas to subsurface earth imaging. This study is focused on the characterization of the non linear wave mixing in rocks at laboratory scale.

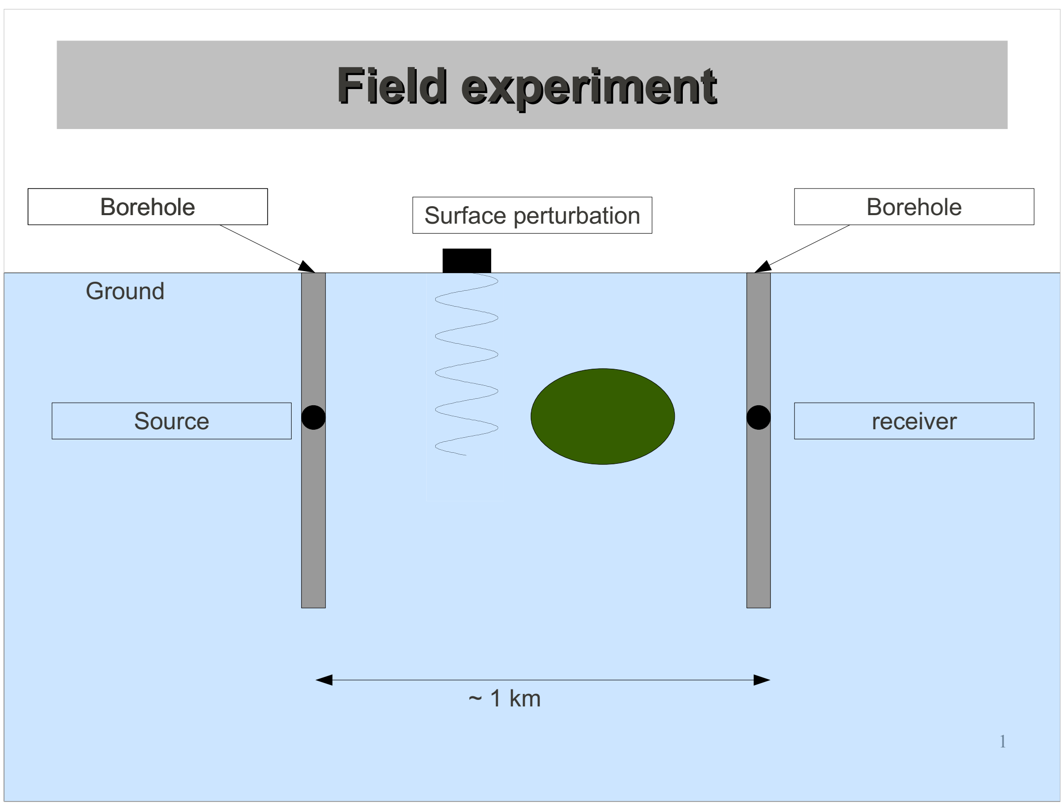

In a borehole configuration, the P-wave speed is measured between a source and receiver embedded into the medium by the boreholes. Then, shear waves are emitted from the surface to perturb the medium, changing the P-wave speed. This perturbation arises from a non-linear wave mixing and can be used to characterize nonlinear parameters of the subsurface.

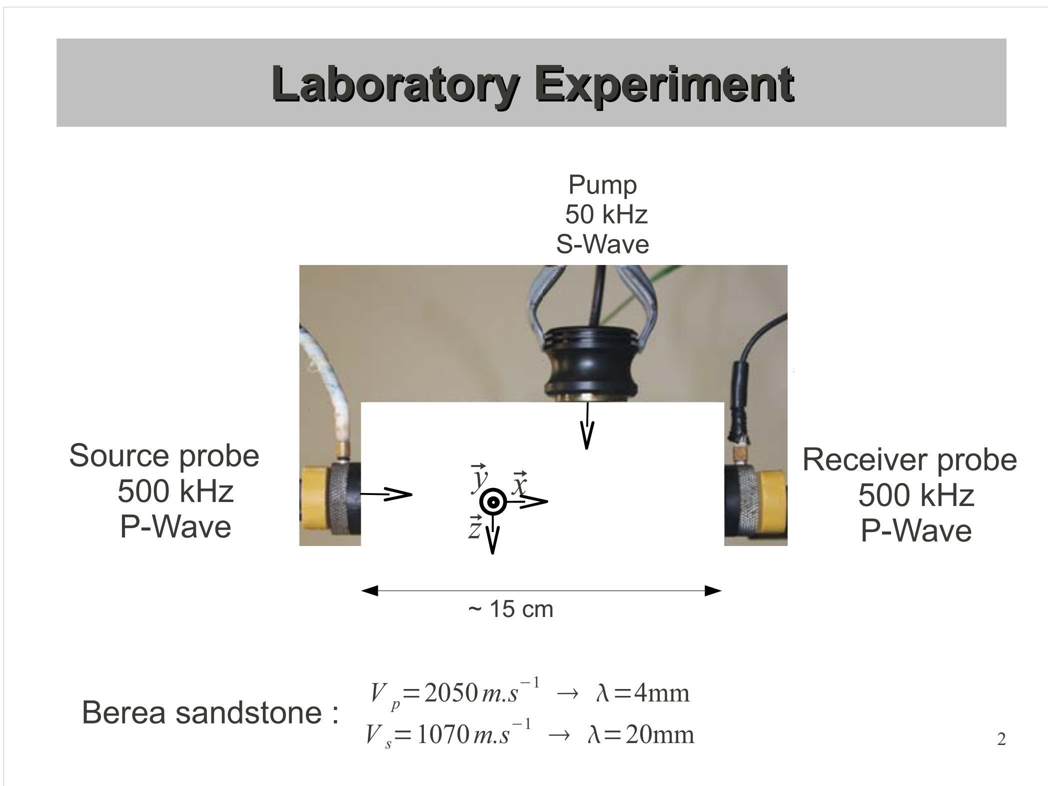

In the laboratory experiment a shear wave transducer is placed on the top of the sample. The s-wave pump will propagate along the z-axis and the p-wave probe along the x-axis. The frequencies are chosen to have a better signal to noise ratio for the probe. The pump frequency is ten times smaller than the probe frequency..

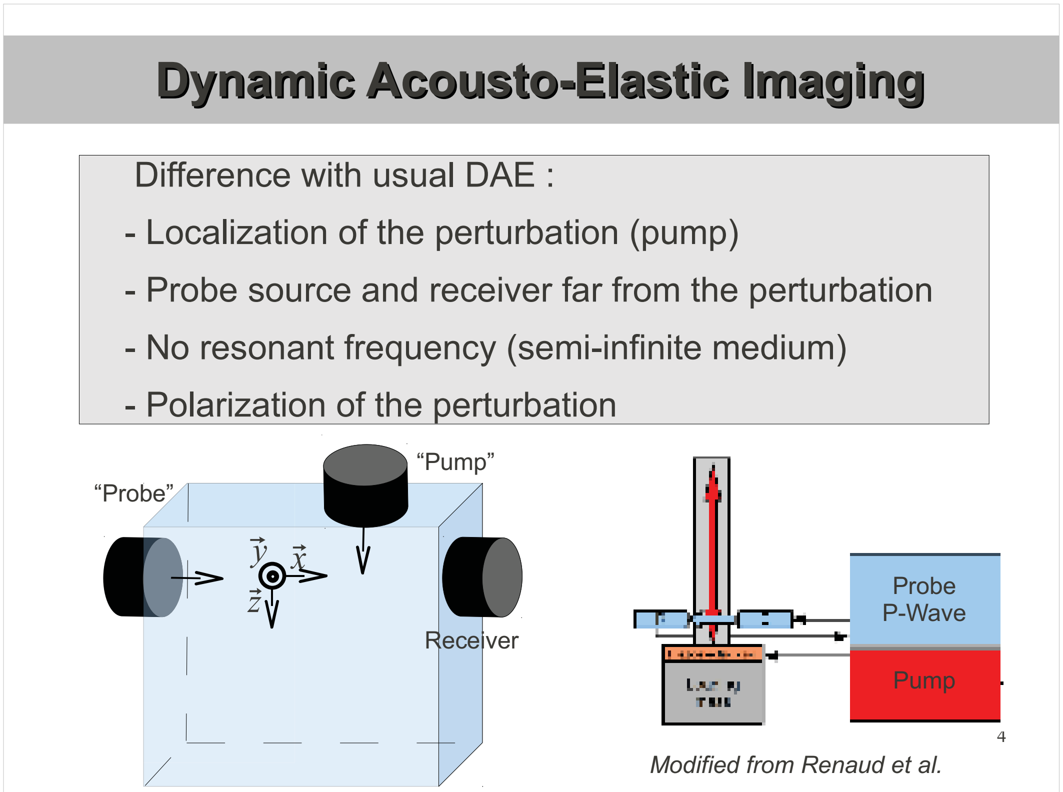

In this standing wave configuration, the experiment is close to the so-called Dynamic AcoustoElastic Testing [1]. A ratio of 10 between probe and pump frequencies ensure a quasi-static strain during the probes' propagation time within the perturbed zone.

The main difference between this method and the DAET method come from the fact that this study is oriented for imaging the medium, not for a global characterization. Consequently the perturbation is localized in order to probe different parts of the medium. Furthermore, the probe and receiver are far from the perturbation, which means that most of propagation path is not perturbed. Finally, S-wave were used for the perturbation.

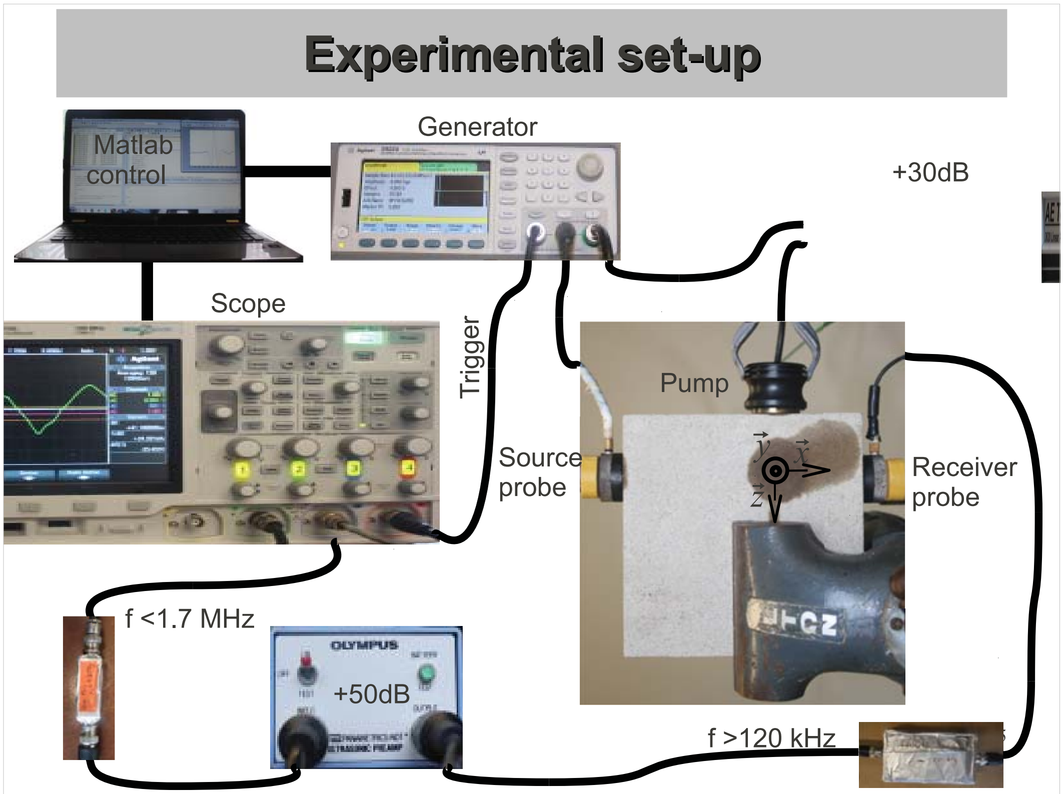

In practice, a generator creates the probe signal, the pump signal and the trigger used to synchronize the scope acquisition. The electronics are fully controlled via Matlab. A power amplifier is needed to reach a sufficiently strong strain in the sample. Then a high-pass frequency filter is used to minimize the amplitude of the pump signal measured at the receiver. The attenuation of the filtering is compensated by a pre-amplifier and finally a low-pass filter eliminates some high-frequency noise.

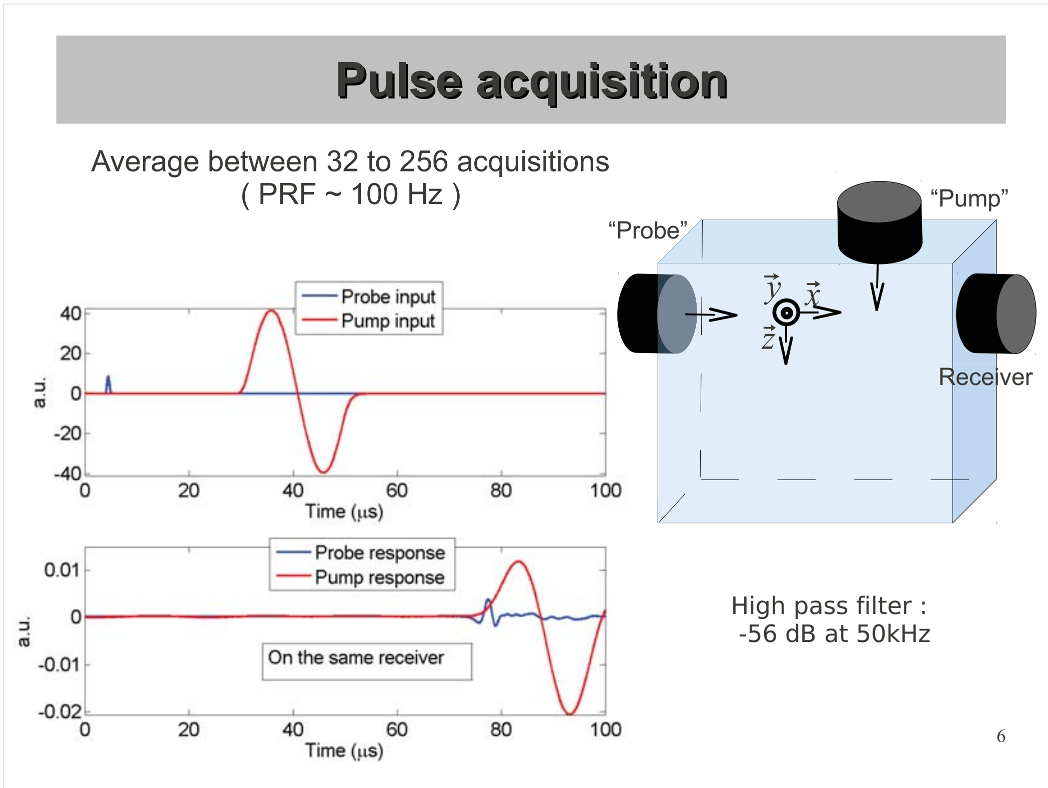

Each measurement is an average of 32 to 256 acquisitions performed by the scope to increase the signal to noise ratio. The Pulse Repetition Frequency (PRF) is chosen to avoid superposition of consecutive signals due to reverberation. Examples of input signals for both probe and pump, and their responses on the same receiver are shown.

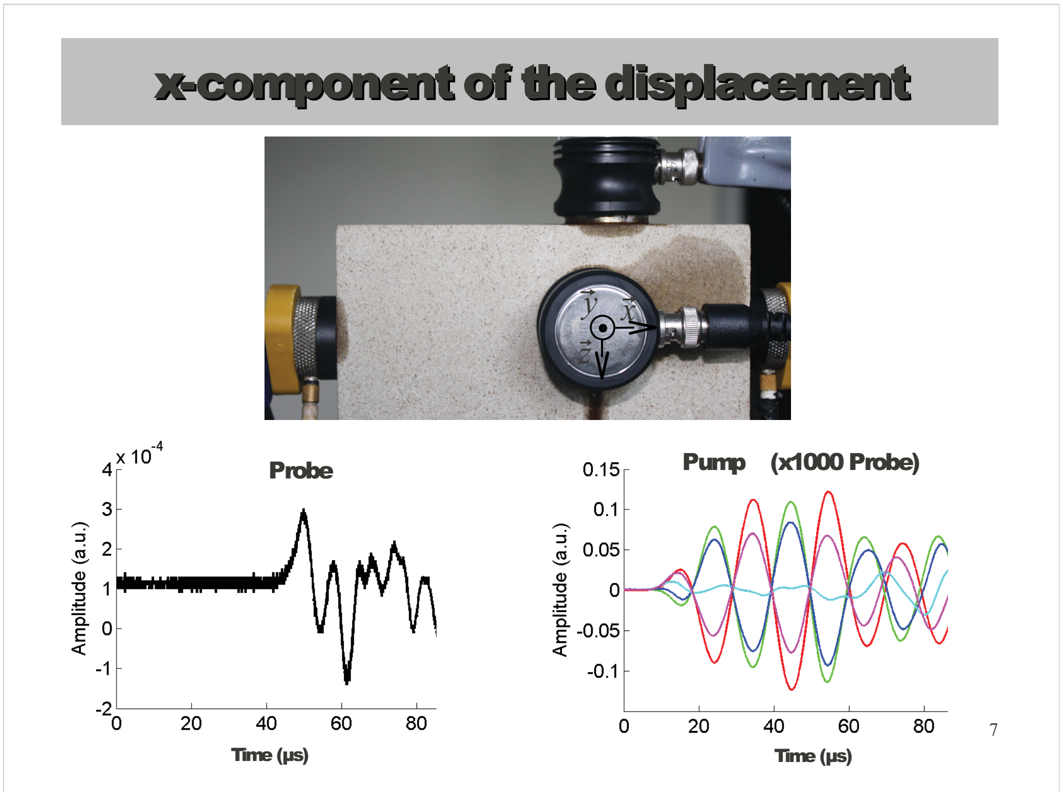

An additional S-wave transducer can be used to measure the x-component of the wavefield at the surface of the sample, around the region of mixing. This measurement shows that the probe amplitude is three orders of magnitude smaller than the pump.

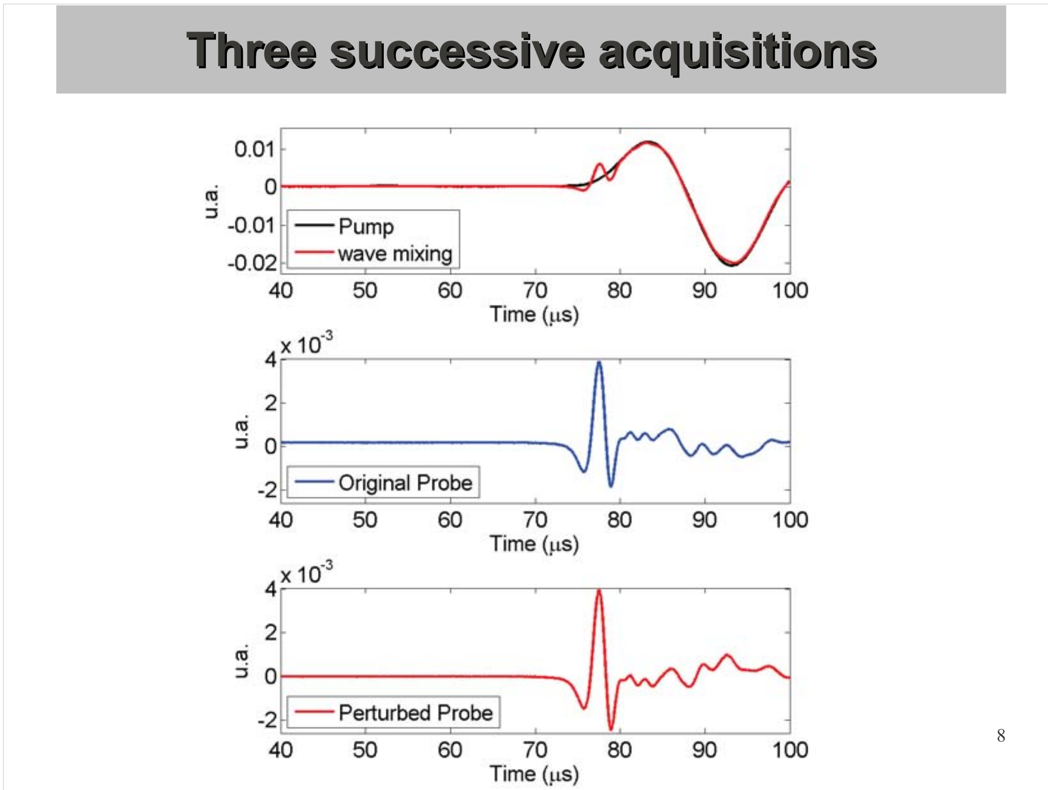

The experimental signals are collected successively: first the probe response is recorded at the probe receiver, then the pump at the same transducer. The phase shift between the two signals can be changed to probe different states of strain within the region of interest.

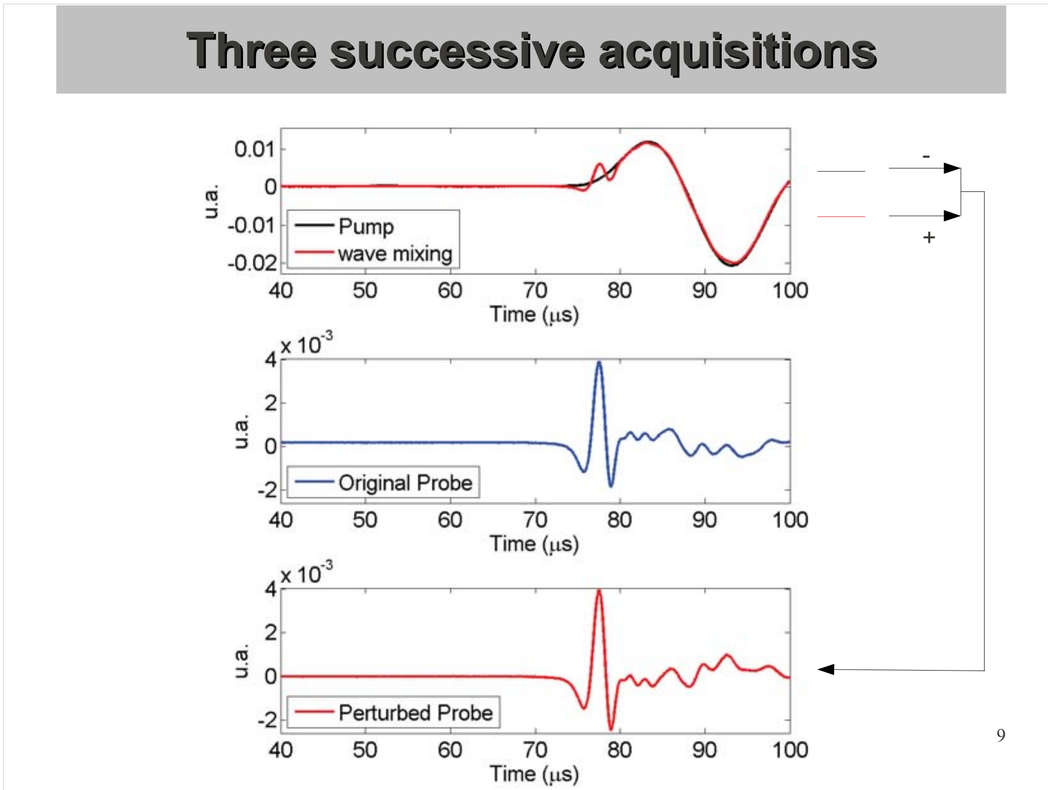

In order to study the effect of the perturbation of the probe by the pump, the signal of the pump alone is subtracted from the wave mixing signal. This step can be considered as an analog filtering of the signal. A perfect synchronization of consecutive acquisitions is needed to ensure a good reconstruction of the perturbed probe. The small variations in both signal emission and triggering are compensated for by repetition and averaging of the measurements.

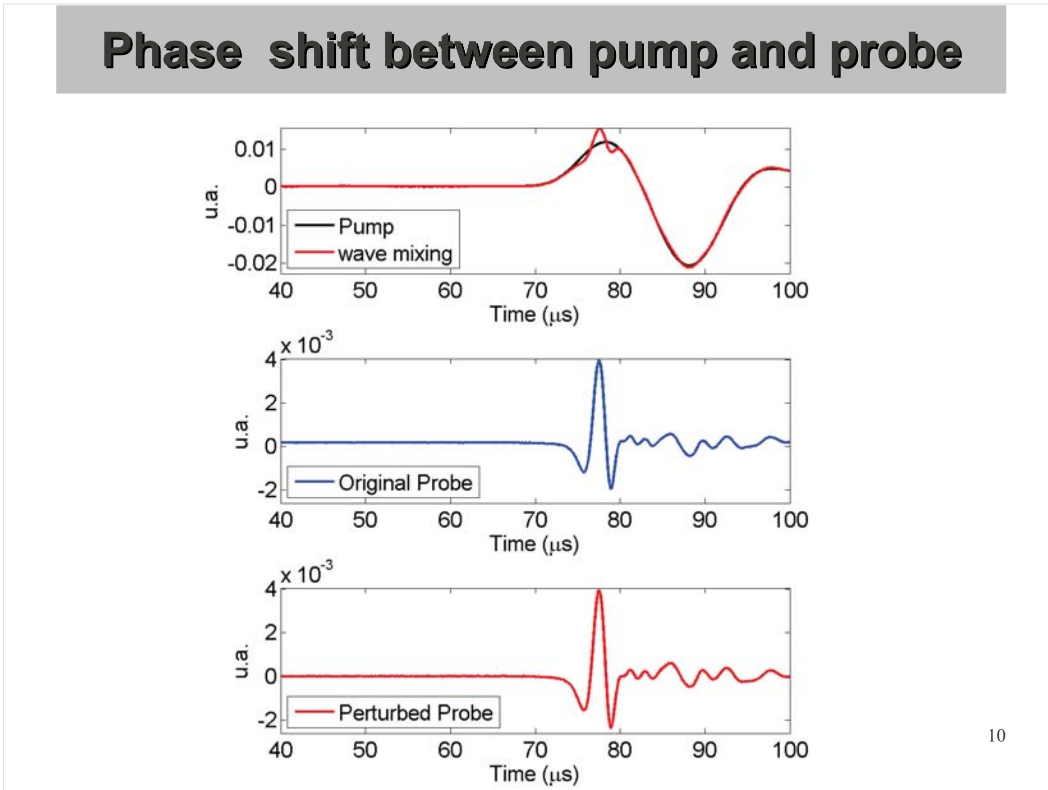

The phase shift between the two signals can be changed to probe different states of strain within the region of interest.

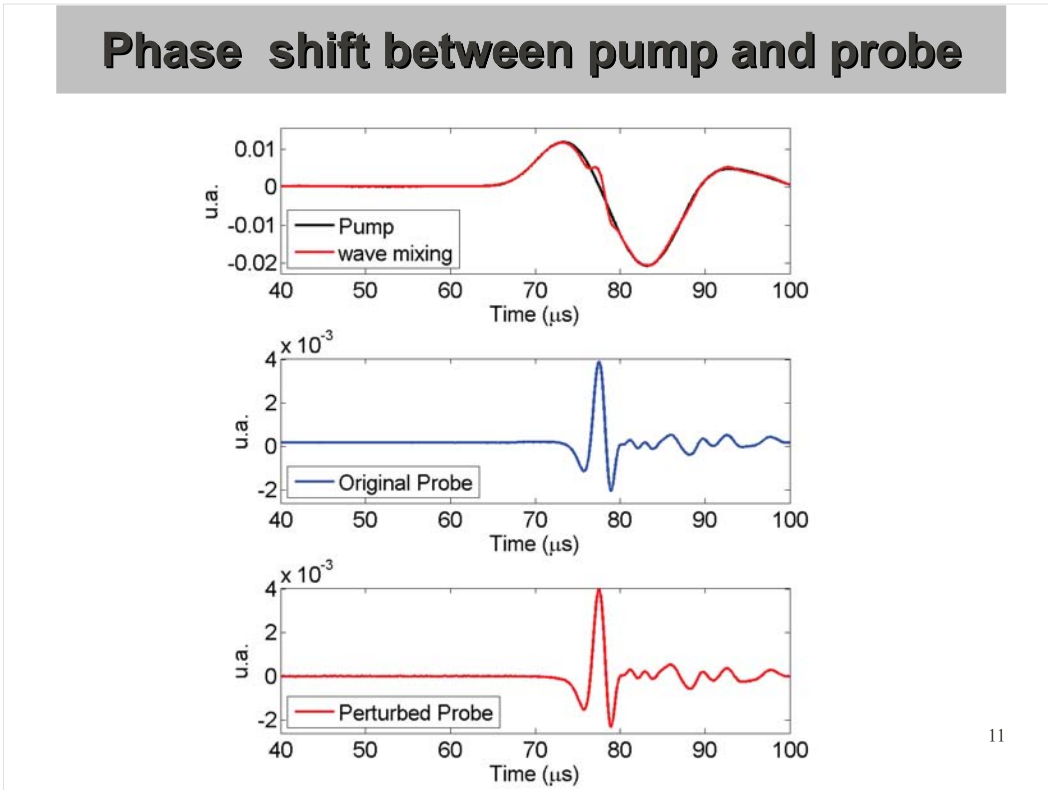
Phase shift between pump and probe
0.01
0
-0.01
-0.02
u.a.
Pump
wave mixing
40 50 60 70 80 90 100
Time (μs)
x 10^-3
4
2
0
-2
u.a.
Original Probe
40 50 60 70 80 90 100
Time (μs)
x 10^-3
4
2
0
-2
u.a.
Perturbed Probe
40 50 60 70 80 90 100
Time (μs)
11

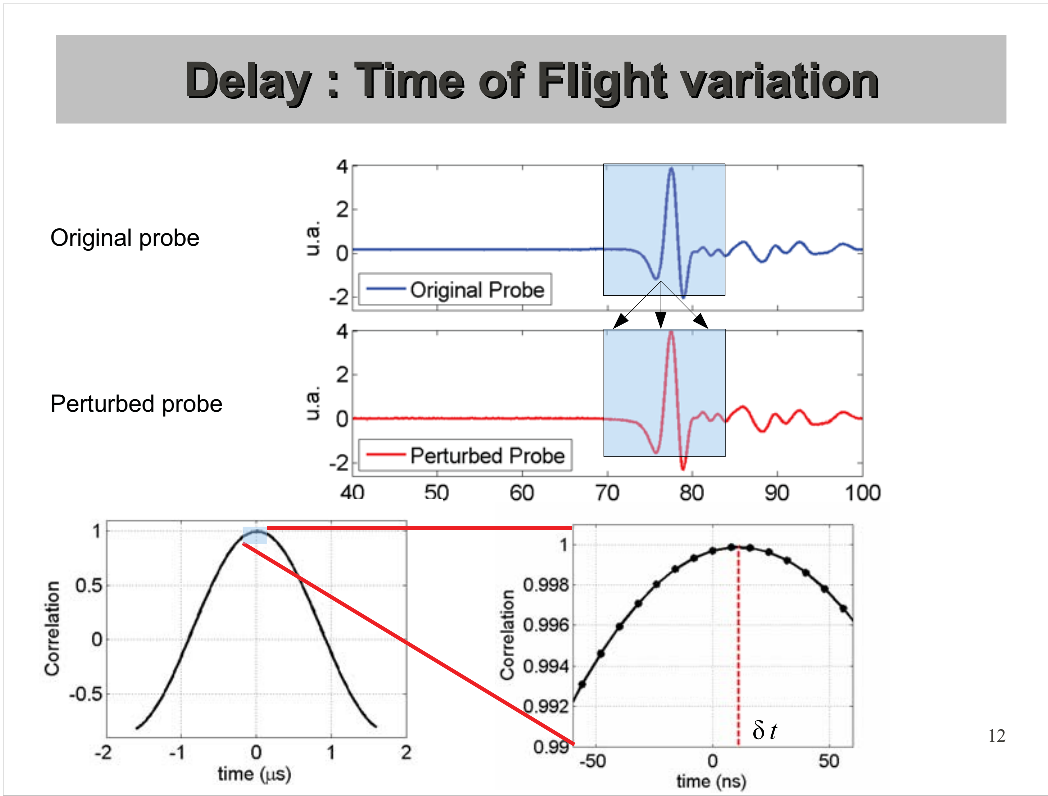

The time perturbation of the probe is studied in the window of the direct wave arrival. To detect small changes in time induced by the interaction of the probe and the pump, the correlation between the original probe and the perturbed probe is computed. To detect sub-sample delays a second order interpolation is performed. The correlation coefficients are very high (~0.99) meaning that the waveform is unchanged. This high coefficient also ensures that the subtraction of the two signal gives a good reconstruction of the perturbed probe.

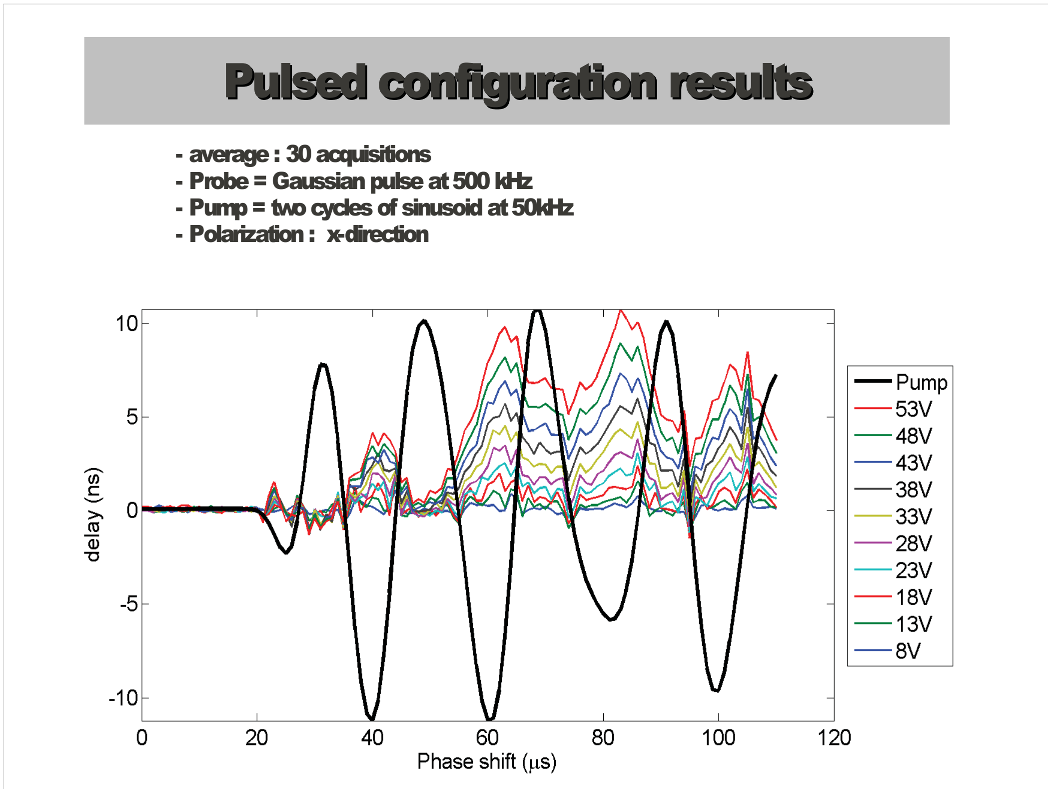

The delays measured between the original and the perturbed probe are represented as a function of the phase shift between probe and pump. The acquisition has been performed for several amplitudes of the pump.

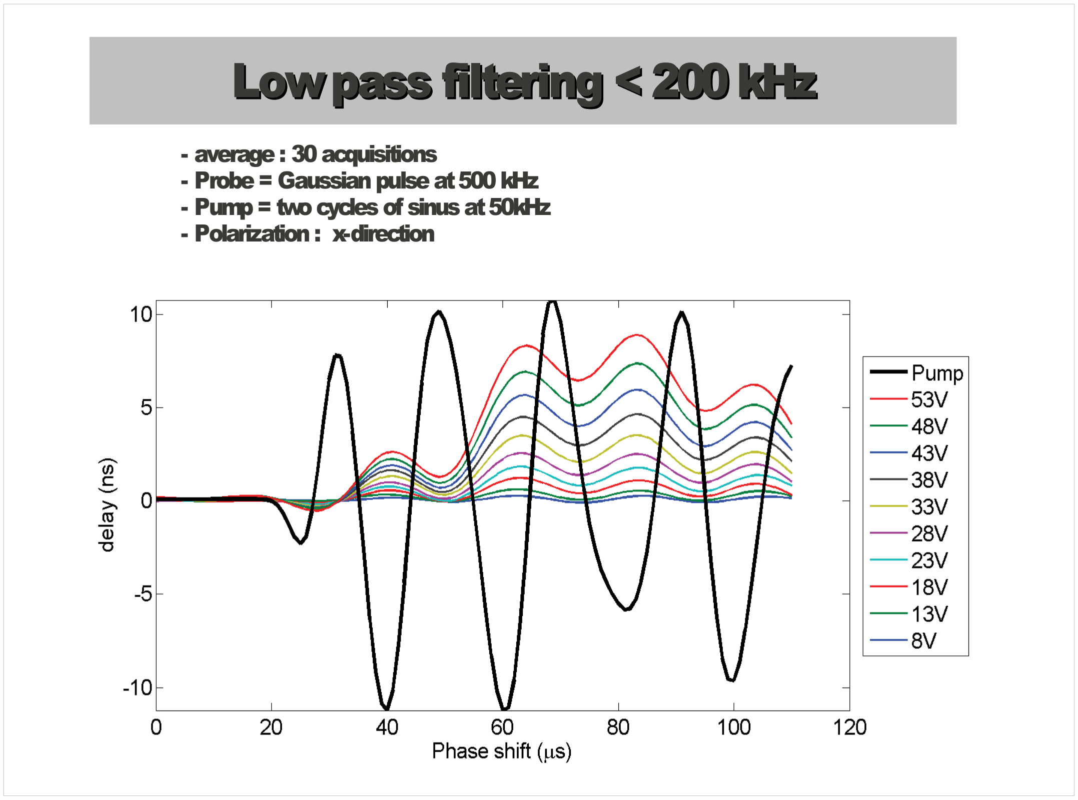

The high frequency signal above 200 kHz is not random noise because it persists when averaging 30 acquisitions. Nevertheless a frequency filtering allows us to focus on the interesting part of the signal. As in the standing-wave case, these results show both fast and slow dynamics.

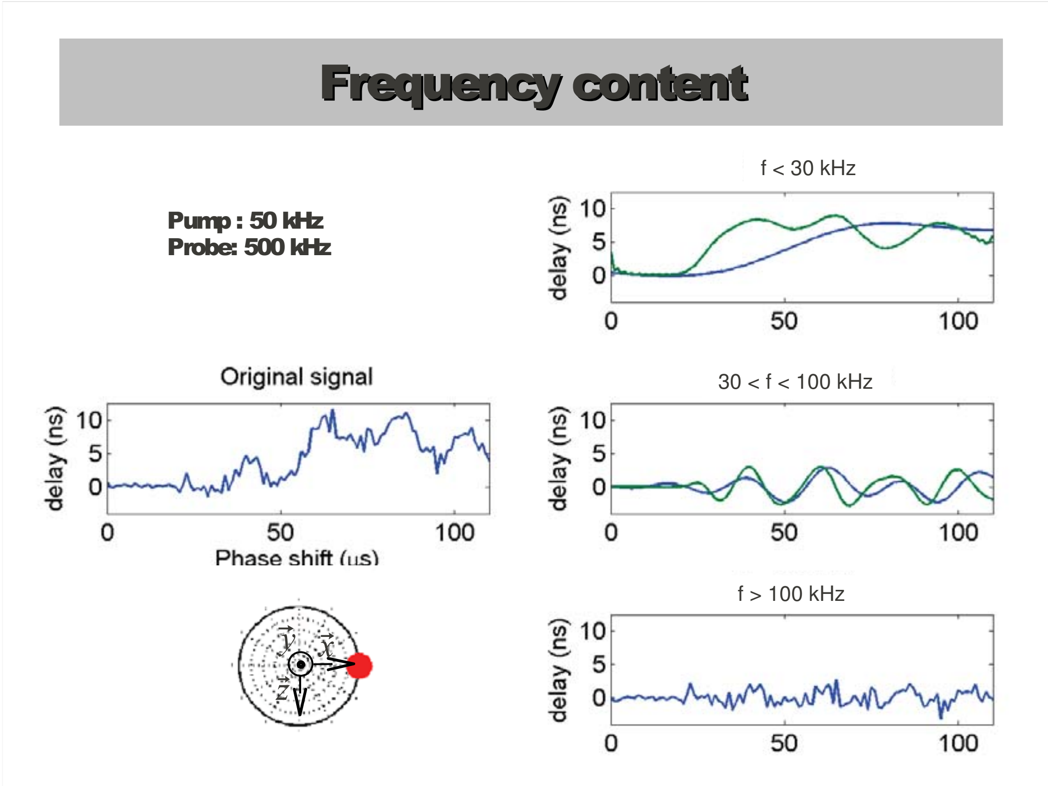

Another frequency filtering is used to study fast and slow dynamics separately. The fast effect directly follows the pump signal. Note that the sign of the pump has been changed since a compression induces a shorter time of flight or a negative delay. On the other hand, the slow effect is delayed by a few cycles of the pump envelope.

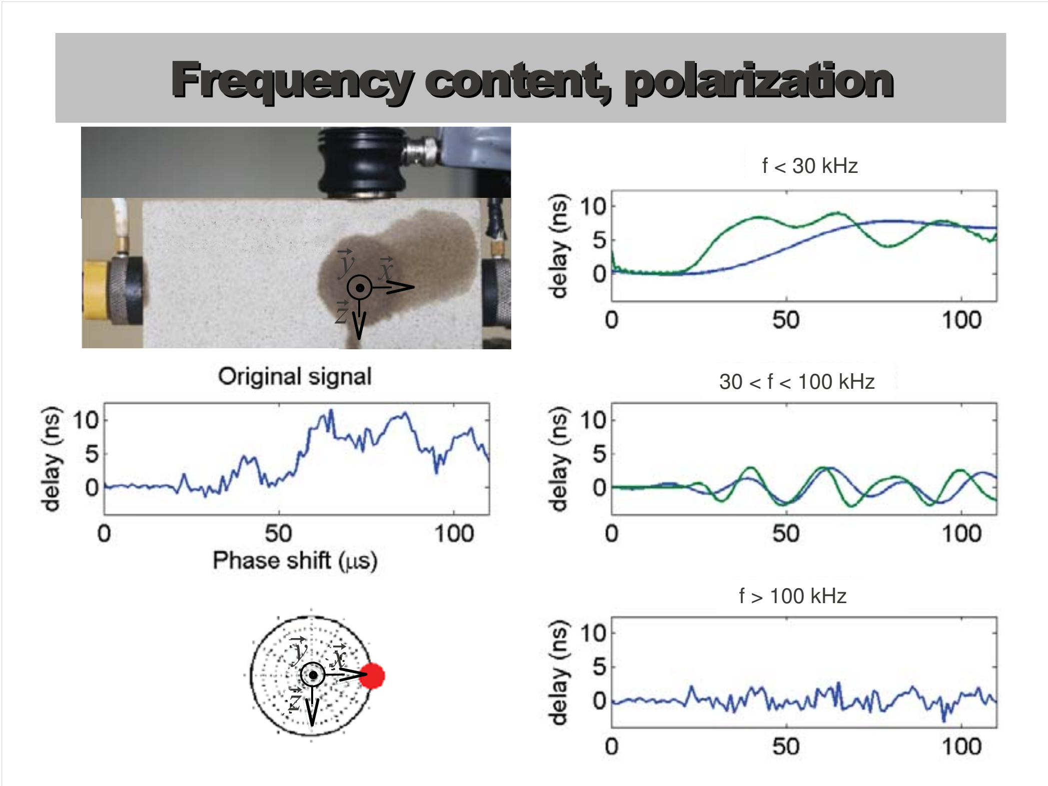

The circle diagram refers to the orientation of the S-wave pump. The red dots shows the direction of the transverse displacement created by the S-wave propagation along the z-axis. In this case, the transverse displacements are along the x-axis.

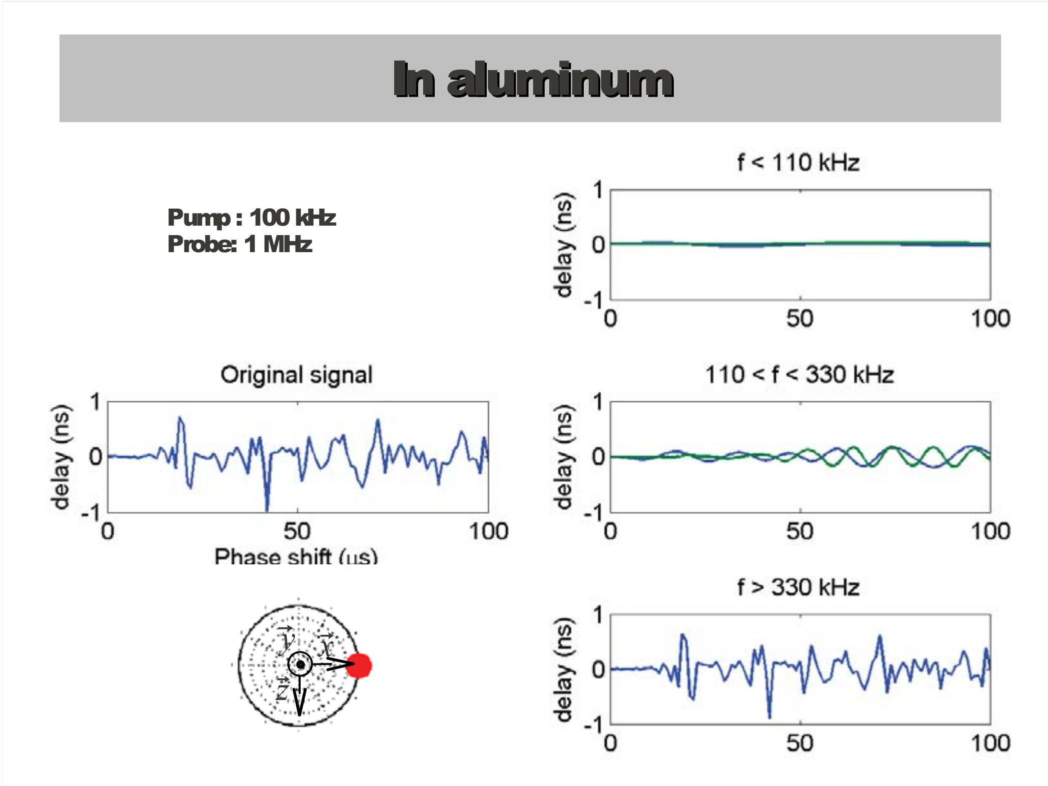

The same experiment has been performed in aluminum. In this case there is no slow dynamic, and a very small fast dynamic effect. Note that the scale of the delays is ten times smaller than before.

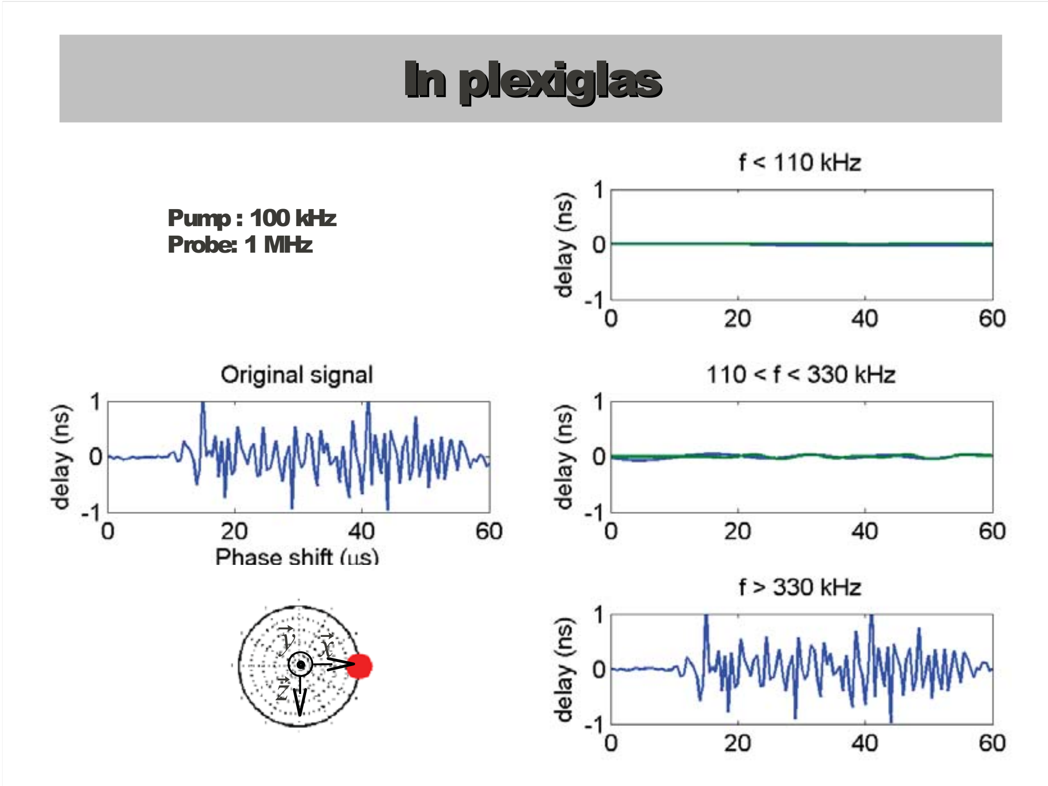

In plexiglass there is no effect that emerges clearly from the noise. These two examples with materials that are known to have small nonlinear behavior illustrate that the method is potentially useful for imaging the nonlinear parameters.

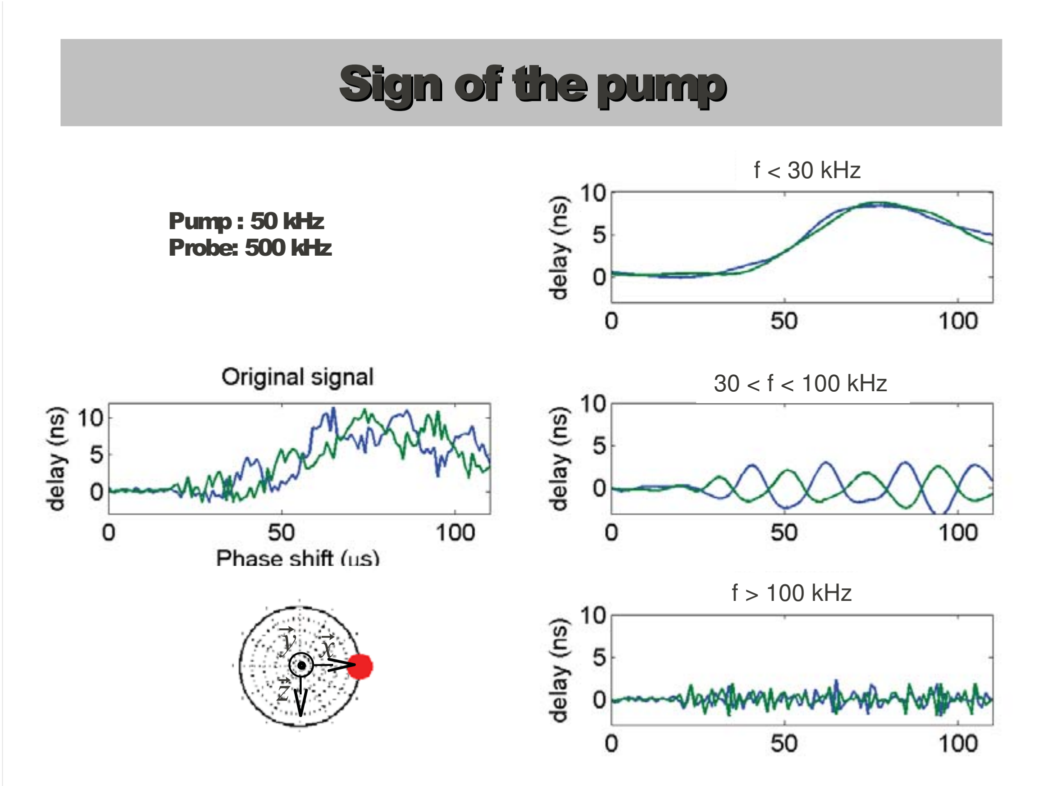

Back to berea, an interesting feature of the two nonlinear effects can be highlighted by changing the sign of the pump. Note that in this plot, the green line does not refer to the pump signal anymore but to the delays measured with a negative pump. The slow nonlinear effect is clearly independent of the sign of the pump, while the fast effect is perfectly the opposite with a negative pump.

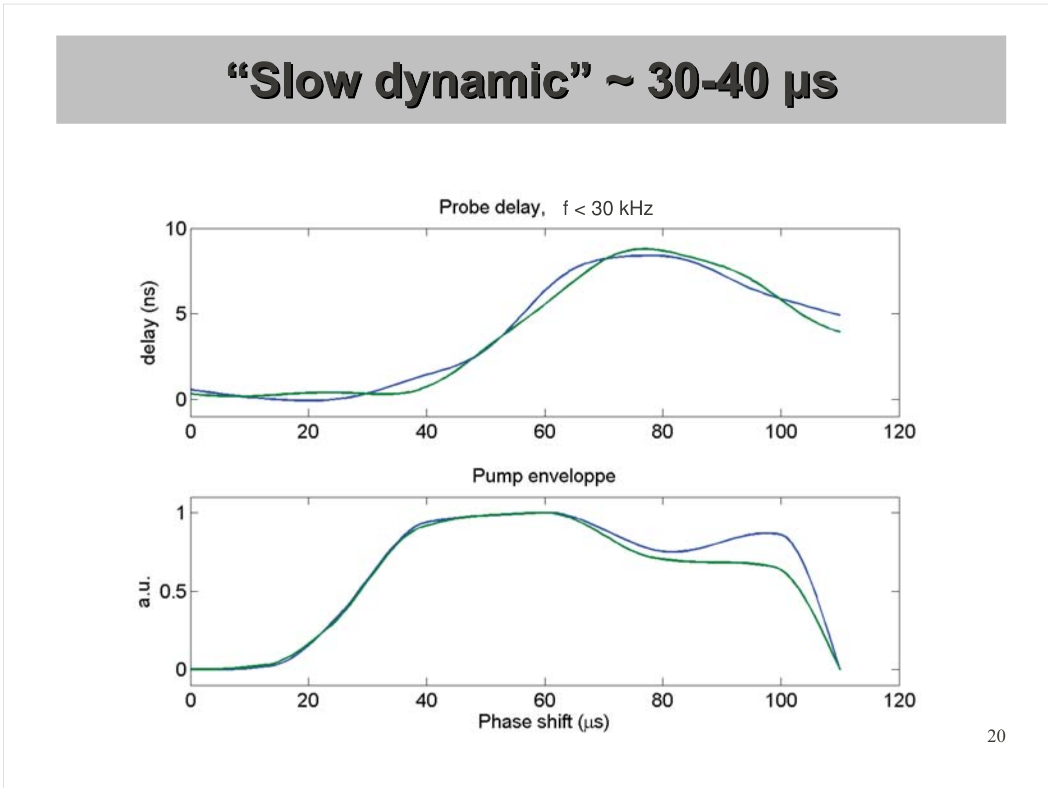

At low frequency, the beginning of the envelopes are identical, this corresponds to the direct arrival of the pump. In this case, the result have to be interpreted carefully because the perturbation are different.

It is interesting to note than the time between the beginning of the perturbation and the nonlinear effect is around 20 microseconds. This is completely different from the time scale of the memory (increasing or decreasing the amplitude) that seen during the first experiment.

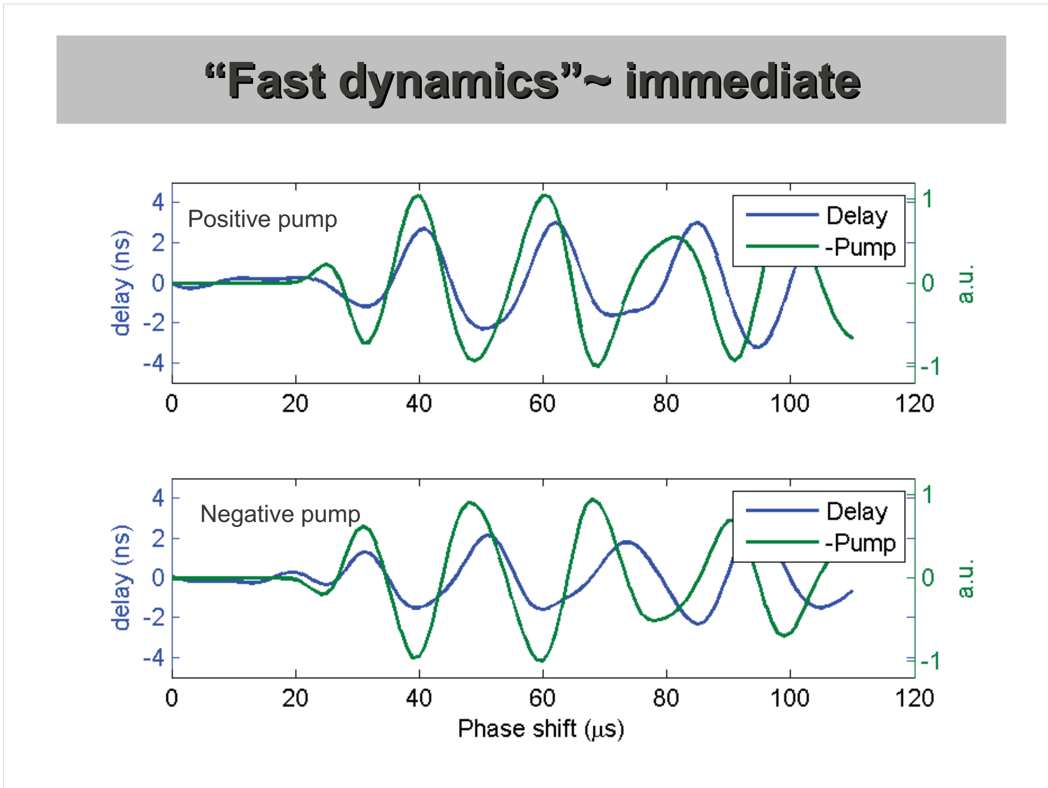

At higher frequency, it is noticeable that only the first two cycles of the delay perfectly follow the negative of the pump signal. These two cycles correspond to the direct arrival of the pump. In this window, there is a small shift of 3 μs between delays and pump because the path of the measured pump and the perturbation are not the same.

A last series of experiment has been performed to study the polarization of the pump, relative to the probe wave direction. In this study it is extremely important to control the coupling between the S-wave transducer and the sample. In this set-up, the coupling is only controlled using a cylindrical weight above the transducer; this enables a rotation of the transducer. A large quantity of S-wave coupling resin was also needed.

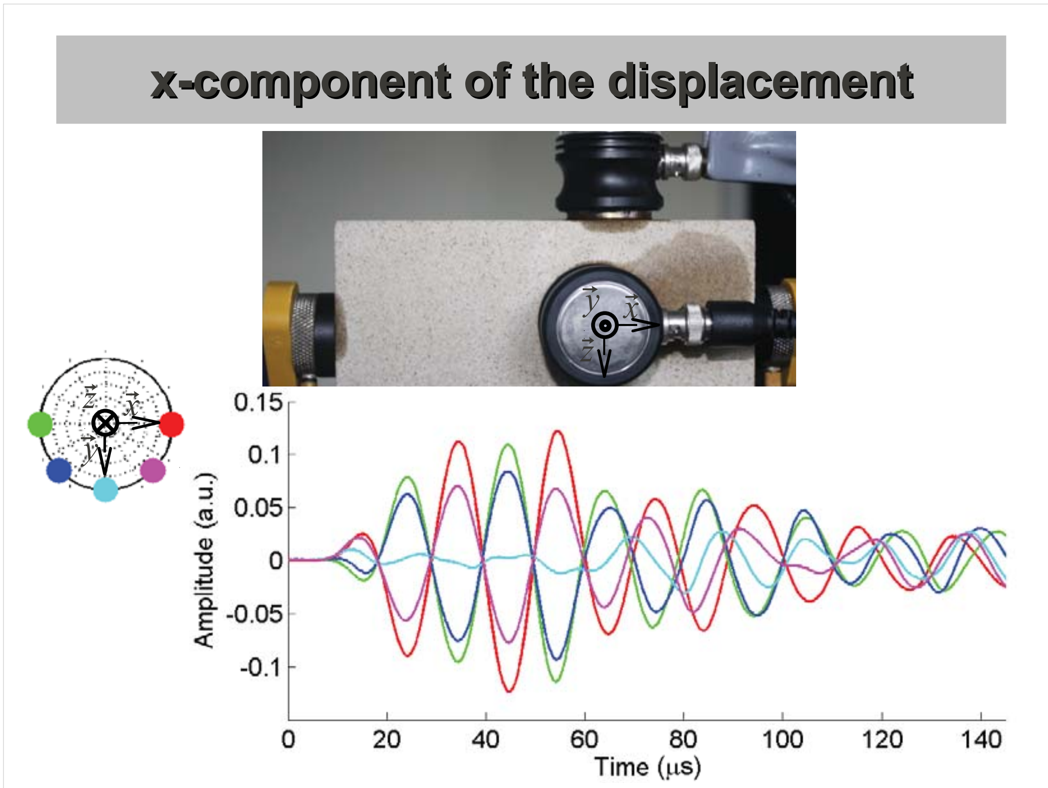

The x-component of the displacement has been measured for different orientations of the transducer. This measurement demonstrates that the coupling is similar for each angle, for example 0° and 180°. At 90° the x-component is very small, as it is supposed to be for a perpendicular component of the S-wave.

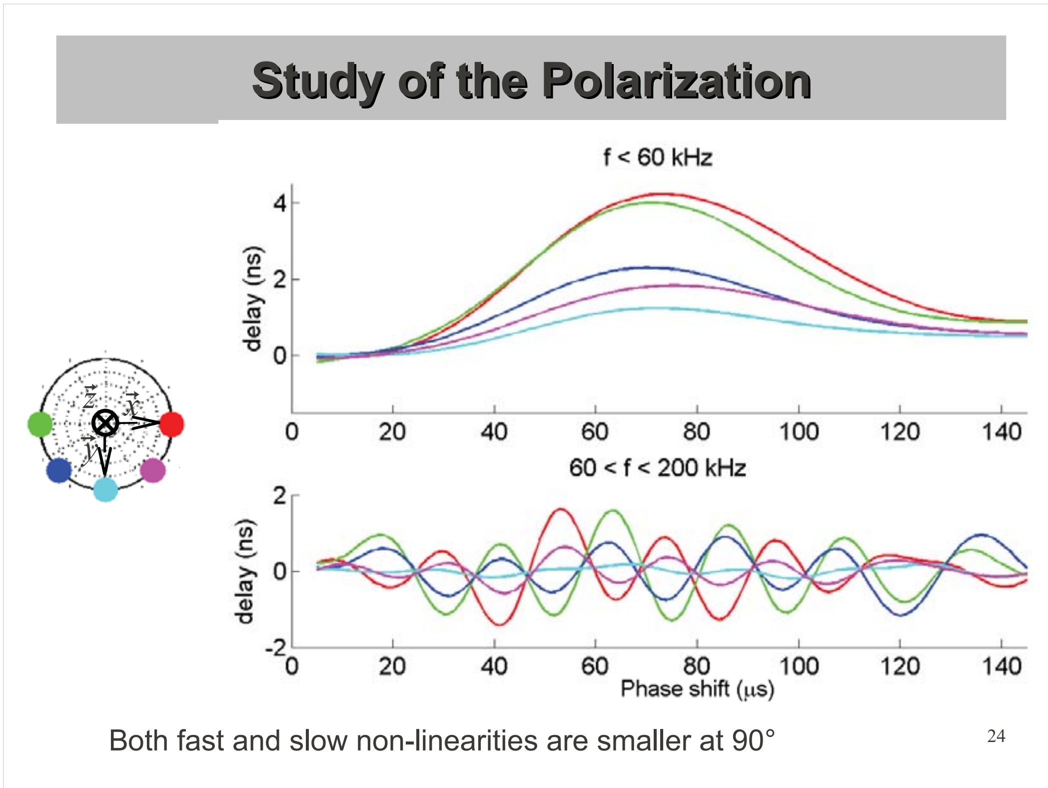

Both fast and slow non-linearities are smaller with a strain oriented along the z axis (perpendicular to the probe wave), but the mechanisms are not the same.On the other hand, the slow effect is smaller because the P-wave is more sensitive to the cracks perpendicular to its path (at least for a compression cf. Ref [2]). An orientation at 90° will more easily open cracks that are parallel to the path.

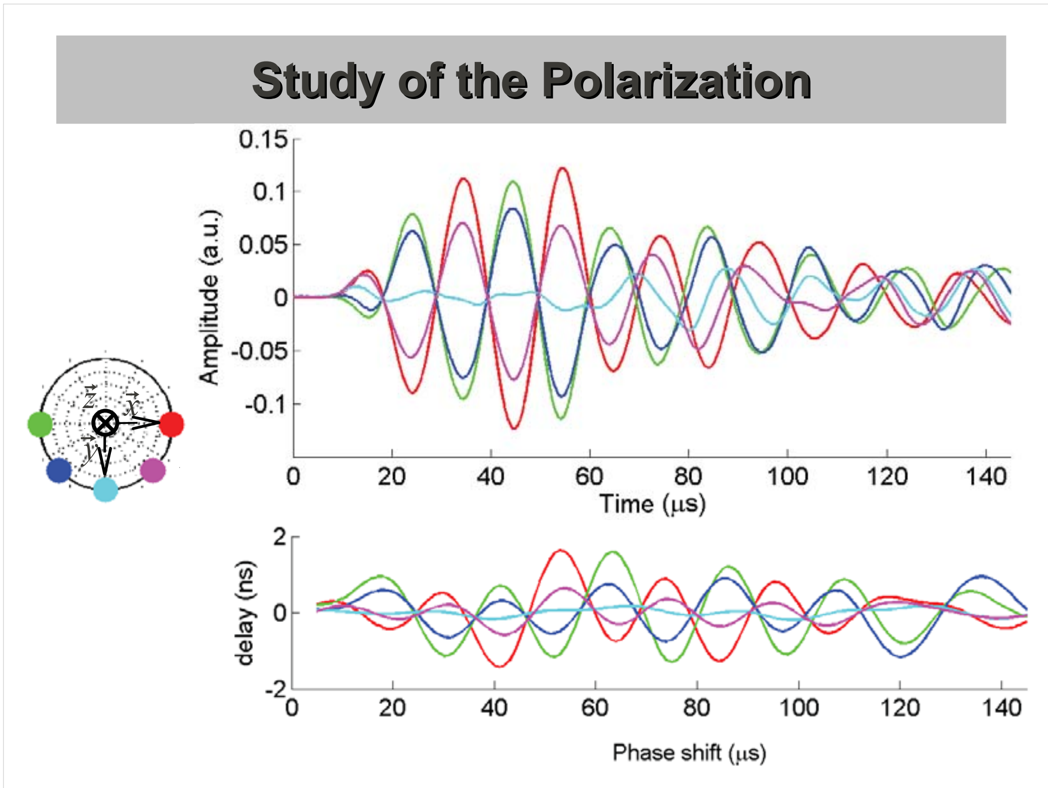

In one hand, the fast dynamic is directly related to the measured strain in the x-axis as shown in the top figure. This effect is clearly related to the quadratic and cubic non-linear parameters.

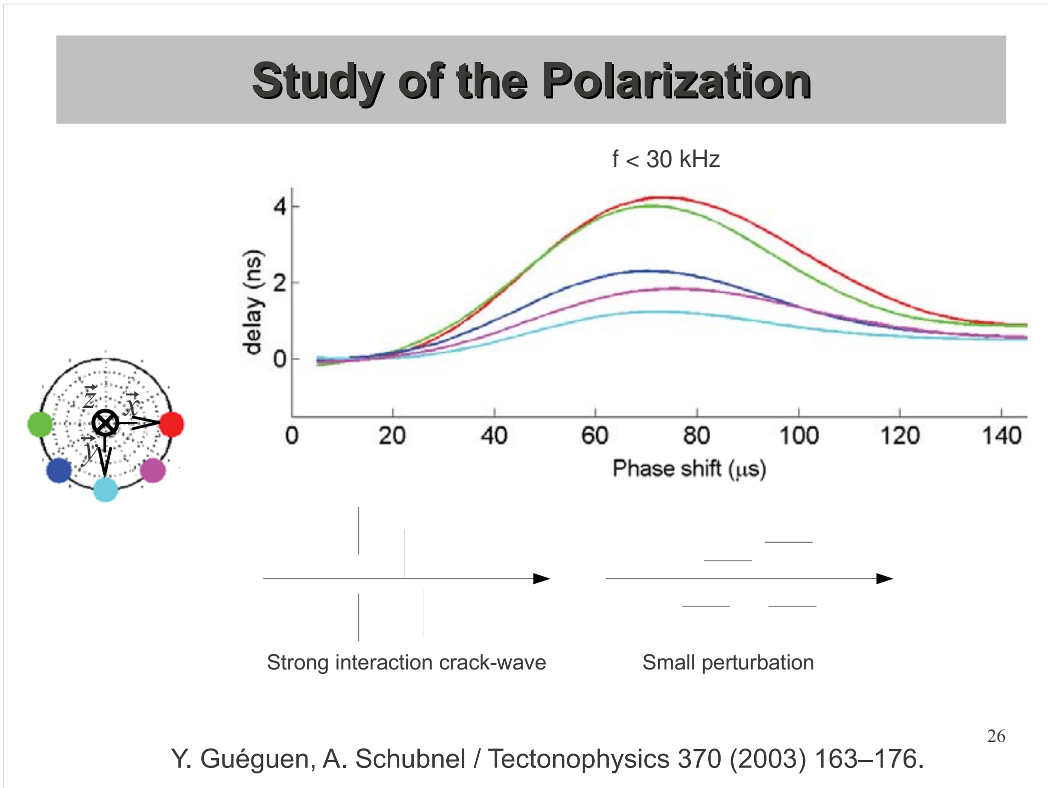

On the other hand, the slow effect is smaller because the P-wave is more sensitive to the cracks perpendicular to its path (at least for a compression cf. Ref [2]). An orientation at 90° will more easily open cracks that are parallel to the path.

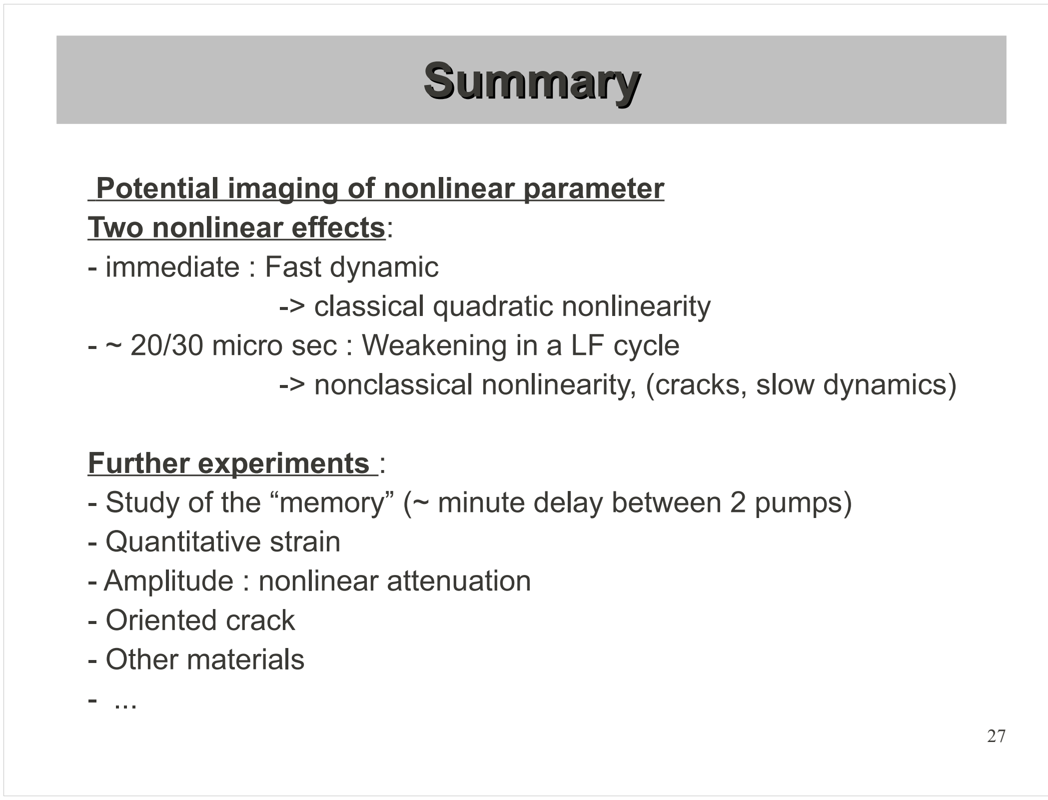

As a summary, we have shown the feasibility of a localized DAET, this opens up the possibility of imaging nonlinear parameters. From a more fundamental point of view, three nonlinear effects have been observed. These three effects can be interpreted as classical, nonclassical nonlinearities and slow dynamics. The link between the two last effect is a subject of current interest. This work remains a preliminary study and many experiments and analysis need to be done in the future.

Acknowledgments

This work was made possible with the funding support of Weatherford. The Authors thank Ingo Geldmacher for helpful discussions.

[1] G. Renaud, S. Callé, and M. Defontaine, "*Remote dynamic acoustoelastic testing: Elastic and dissipative acoustic nonlinearities measured under hydrostatic tension and compression*", A.P.L. 94, 2009.

[2] Y. Guéguen, A. Schubne, "*Elastic wave velocities and permeability of cracked rocks*", Tectonophysics 370, 2003.